




Palladium-containing catalysts based on mesostructured material of the cmk type in the reaction of oxygen electroreduction

Evgenia A. Martynenko¹ · Sergey V. Vostrikov¹ · Roman V. Shafigulin²  · Kirill Yu. Vinogradov² · Elena O. Tokranova² · Andzhela V. Bulanova² · Hong Zhu³

Received: 22 February 2022 / Accepted: 10 November 2022 / Published online: 28 November 2022
© The Author(s), under exclusive licence to Springer Nature B.V. 2022

Abstract

Palladium-containing ordered mesoporous carbons, such as CMK-1 and CMK-3 doped with nitrogen by pyrolysis of polyaniline and modified with an imidazolium ionic liquid ([BMIM][Br]) have been synthesized. The carriers and electrocatalysts have been studied by low-temperature nitrogen adsorption, thermogravimetric analysis, X-ray fluorescence analysis, and Raman spectroscopy. A significant decrease in the surface of CMK materials was shown upon doping with nitrogen and modifying with an ionic liquid. Moreover, the electrocatalytic activity in the oxygen reduction reaction from an alkaline electrolyte has been studied by the potentiometric method using a three-electrode cell with a rotating disk as working electrode. In addition, the diffusion currents, half-wave potentials, initial potentials, and the number of electrons participating in the reaction are calculated. The values of the electrochemical active surface of the synthesized catalysts were determined on the basis of cyclic voltammograms. Modification CMK-3_Pd with ionic liquid made it possible to increase the diffusion current, which was not observed upon doping with nitrogen. Catalysts CMK-3_Pd and CMK-3_Pd_IL showed high efficiency in the reaction under study. The number of electrons transferred during the electroreduction of oxygen on these catalysts is about 3.5; mass activity in the diffusion region at a potential of -0.8 V is about 0.7 A/mgPd; and it is almost two times higher than that of the commercial platinum Pt/C catalyst. In the kinetic region at a potential of -0.05 V, the specific activity of the platinum catalyst is significantly higher than that of CMK-3_Pd and CMK-3_Pd_IL. Mass activity in the kinetic region for CMK-3_Pd and CMK-3_Pd_IL is comparable to the activity of the Pt/C platinum catalyst. It was shown that the activity of materials based on CMK in the reaction of oxygen electroreduction from an alkaline electrolyte will depend not only on the size of the electrochemically active surface of the catalysts, but also on the textural characteristics of these materials.

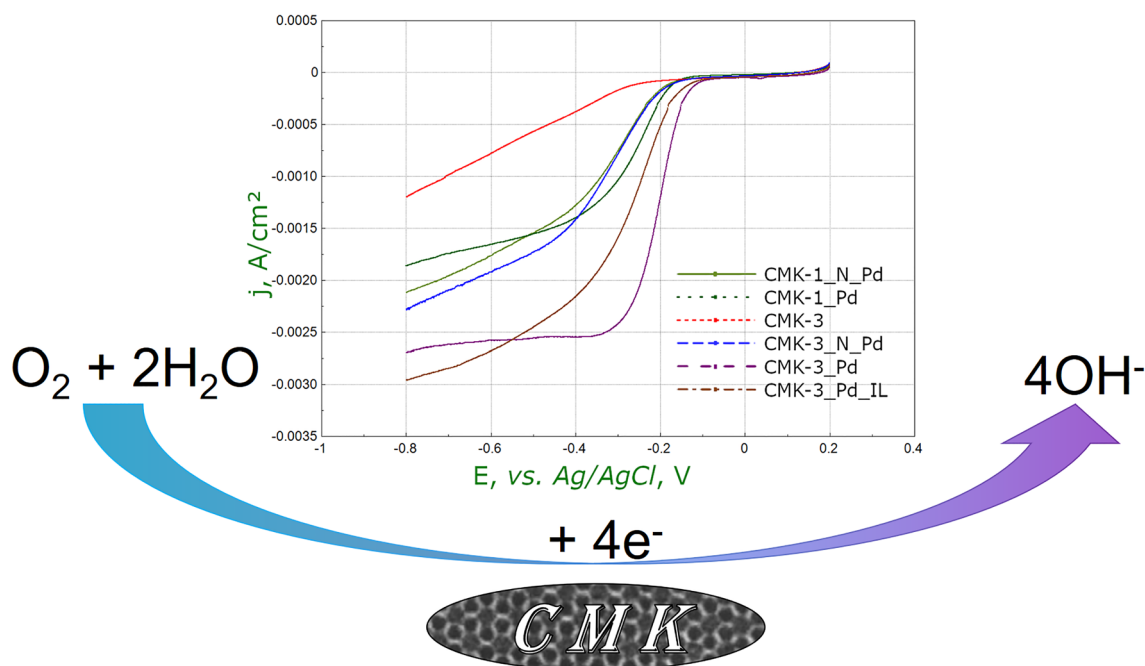
✉ Roman V. Shafigulin
shafiro@mail.ru

¹ Samara State Technical University, 443100 Samara, Russia

² Institute of Natural Sciences, Samara University,
443086 Samara, Russia

³ Institute of Modern Catalysis, Beijing University of Chemical
Technology, Beijing, People's Republic of China

Graphical abstract



Keywords Electrocatalysts · Mesoporous carbons · Oxygen reduction from an alkaline electrolyte · Palladium catalysts · Doping with nitrogen · Modification with an ionic liquid

1 Introduction

Currently, an active search is underway for environmentally friendly, economically viable, efficient systems for the conversion, and storage of alternative energy. Membrane fuel cells are in the focus of scientific research as potential energy sources for stationary and mobile applications [1, 2], but expensive platinum-based electrocatalysts remain their main barrier [3–6].

Therefore, in recent years, much effort has been made to develop highly efficient catalysts that will demonstrate comparable or even higher catalytic activity than Pt. A number of strategies have been proposed, such as the synthesis of Pt–Me (where Me is any metal) binary catalysts [7, 8] or the replacement of platinum with other metals. Thus, electrocatalysts based on palladium [9, 10], iron [11, 12], nickel [13, 14], copper [15], and other metals have been investigated. Some researchers focus on the study of binary and ternary alloys, such as, for example, Ni–Co [16], Ni–Mo [17], and Fe–Co–Ni [18]. However, the developed catalysts still have a lower activity than platinum materials; moreover, they are susceptible to corrosion and oxidation in electrolytic environments.

Another strategy for reducing the cost of catalysts is the use of new carbon supports, which will improve the

dispersion of metal nanoparticles and, thus, increase the activity of the catalyst. Ordered mesoporous carbons (OMCs) have generated wide research interest due to their high specific surface area, large pore volume, high electrical conductivity, chemical stability, and low cost [19, 20]. In general, the ability to control the properties of OMC such as surface area and pore size, combined with possibility of doping with metal nanoparticles and heteroatoms, makes this class of carbon materials suitable for studies of electrocatalytic processes.

Among the whole variety of mesoporous carbons, it stands out the CMK family (Carbons Mesostructured by Korea Advanced Institute of Science and Technology) based on mesostructured silicon oxides. These OMCs have been widely studied in the literature as promising catalysts for redox reactions. These OMCs have a highly ordered three-dimensional cubic structure (CMK-1) and a hexagonal structure (CMK-3). Interconnected channels provide a large pore volume, which facilitates the diffusion of oxygen and the transfer of reagents to the active sites of the catalyst [21, 22].

Doping of carbon materials with heteroatoms can additionally modify the electronic and physicochemical properties of OMC [23, 24]. For example, doping with elements such as nitrogen and sulfur increases the electron density, which can facilitate oxygen adsorption and diffusion and

effectively weaken the O–O bond. Studies show that catalysts based on CMK-3 doped with nitrogen atoms have high activity and stability [25].

In recent years, the use of ionic liquids in electrochemistry, and in catalysts for the electrochemical reduction of oxygen for fuel cells, has been actively studied. The use of ionic liquids as precursors makes it possible to specify a certain structure of the active site, for example, a metal surrounded by several nitrogen atoms [26] or to influence the textural characteristics of electrocatalysts [27].

In the present study, palladium-containing catalysts based on ordered mesoporous carbon materials CMK-1 and CMK-3, doped with nitrogen and modified with an ionic liquid were synthesized.

The aim of the work was to investigate the electrocatalytic activity of the obtained materials in the reaction of oxygen electroreduction from an alkaline electrolyte using a rotating disk electrode in linear and cyclic voltammetry modes.

2 Experiment

2.1 Catalyst synthesis

The synthesis of mesoporous carbon materials was carried out by the template method. Mesoporous silicates synthesized by presented methods: MCM-48 [7] and SBA-15 [6], respectively, were used as templates for the preparation of CMK-1 and CMK-3. To obtain mesoporous carbons, the synthesized samples of silicate materials were twice impregnated with an aqueous solution of sucrose containing sulfuric acid, similarly to the procedure described in [3]. Carbonization was completed by pyrolysis with heating to 600 °C in a nitrogen atmosphere. The resulting carbon-silicate composite was treated with an HF solution at a temperature of 50 °C for 3 h to remove the silicate template. Then the material was filtered, washed with ethanol, and dried at 120 °C. The obtained carbon materials were designated using the international nomenclature based on MCM-48—CMK-1, SBA-15—CMK-3.

When preparing N-doped samples, the technique described in [25] was used. A 30 mg of carbon was dispersed in 10 mL of deionized water with sonication for 10 min. Then, a 300 µL of aniline and 1500 µL of an aqueous solution of HCl (2 M) were mixed at room temperature, and the resulting mixture was added to a dispersed solution with carbon and stirred with ultrasound for 5 min. A 1350 mg FeCl₃·6H₂O was added to the above mixture (the molar ratio of aniline to FeCl₃ was 2: 3), which initiated the oxidative polymerization in situ. The mixture was kept on an ice bath for 24 h with stirring. The resulting composite was a green dark precipitate, which was separated by centrifugation and washed 3 times with deionized

water and ethanol. Then, the samples were dried in vacuum at 60 °C and heated in an N₂ atmosphere at 900 °C with a heating rate of 5 °C min⁻¹ for 2 h. The resulting composites were designated CMK-1_N and CMK-3_N, respectively.

For the preparation of palladium-containing catalysts, the active component (~ 5 wt%) was applied to N-doped and undoped carbon supports by the method of single incipient wetness impregnation. Palladium chloride PdCl₂ (99.995%, CAS 7647-10-1, Merck) was used as a precursor. The impregnated samples were kept for a day at room temperature, and then dried at 60 °C for 6 h and calcined at 200 °C on air for 1 h. The reduction of the catalysts was carried out in a stream of hydrogen at 350 °C for 2 h. The resulting composites were designated as CMK-1_N_Pd, CMK-3_N_Pd, CMK-1_Pd, and CMK-3_Pd.

The palladium-containing catalyst was modified with an ionic liquid by the method of single impregnation. As the ionic liquid, an imidazolium ionic liquid [BMIM] [Br] was used. A sample of a palladium-containing catalyst impregnated with an ionic liquid was sonicated for 5 h and then dried at 100 °C on air. The resulting composite was designated CMK-3_Pd_IL (5 wt% Pd, 23 wt% IL).

2.2 Characteristics of catalysts

The textural characteristics of the synthesized supports and catalysts were studied by low-temperature nitrogen adsorption using a Quantochrome Autosorb-1 porosimeter (Quantochrome instruments). The specific surface area was calculated using the Brunauer–Emmett–Teller (BET) model.

The qualitative analysis was carried out by the method of X-ray fluorescence (XRF) analysis on a BRA-18. The Raman analysis was performed under backscattering geometry on a Renishaw InVia micro-Raman spectrometer equipped with a Charged Coupled Device (CCD) detector, Ar-ion laser ($\lambda = 532$ nm), and 1800 lines/mm grating with a spectral resolution of 1 cm⁻¹. The excitation source was focused down to a 2 µm spot with a laser power of about 1 to 5 mW.

The thermoprogrammed reduction of catalysts was carried out on a TPDRO 1100 instrument using a thermal conductivity detector. The reduction process was carried out in a mixture of 5% hydrogen volume in nitrogen with the following parameters: volumetric flow rate 50 mL/min, temperature range from room temperature to 1100 °C, and heating rate 10 °C min⁻¹. Directly before analysis, the samples were dried in an argon atmosphere.

Thermogravimetric analyses were performed on an STA 449 F3 Jupiter (NETZSCH) instrument in the temperature range from 35 to 800 °C at a heating rate of 10 °C min⁻¹ in an air flow with a flow rate of 200 mLmin⁻¹.

2.3 Electrochemical measurements

2.3.1 Preparation of catalytic ink

The 0.02 g of the catalyst was dissolved in 5 mL of ethyl alcohol and 250 μL of Nafion's solution (5 wt%), and then the resulting solution was ultrasonicated for 2 h in an Ultrasonic disperser. After that, the catalytic ink was applied to the surface of a glassy carbon (GC) disk electrode (electrode surface area 0.071 cm^2) with a pipette at a load of 80 $\mu\text{g cm}^{-2}$ and dried for 4 h at a temperature of 90 $^\circ\text{C}$ on air. A catalytic ink based on commercial platinum on carbon [metal content 20%—(Pt/C)] was prepared in a similar way. This catalyst was used for comparative analyses.

2.3.2 Electrochemical measurements

The oxygen reduction reaction from alkaline solutions was studied by the potentiometric method using an electrochemical workstation «CorrTest» in the modes of cyclic and linear voltammetry (LV). A three-electrode cell with a rotating disk working electrode was used. A platinum electrode with a large surface was used as an auxiliary electrode, and a silver chloride electrode served as a reference electrode. The oxygen reduction reaction was studied in a 0.1 molar potassium hydroxide solution. Linear voltammograms were recorded in an air-saturated potassium hydroxide solution in the potential range of « $-800 \div 200$ mV» with a potential sweep of 5 mV s^{-1} and at various speeds of rotation of the working disk electrode (500–3000 rpm). Cyclic voltammograms (CV) were recorded in a de-aerated atmosphere in the potential range of « $-1000 \div 200$ mV»

3 Results and discussion

3.1 Physicochemical studies of samples

Nitrogen adsorption–desorption isotherms and pore size distribution for synthesized CMK-1 and CMK-3 carbon supports are shown in Fig. 1. The isotherms are type IV (IUPAC classification) with a typical H1 hysteresis loop at a relative pressure (P/P_0) 0, 45–0.9, which corresponds to capillary condensation inside the pores [28] and indicates the mesoporous nature of the prepared samples.

As shown in Table 1, the obtained mesoporous coals are characterized by very high values specific surface area (S_{BET}). This is due to the large number of micropores

Table 1 Textural characteristics of synthesized carbon materials and catalysts

Sample	Surface area S_{BET} , $\text{m}^2 \text{g}^{-1}$	Pore volume, V_p , $\text{cm}^3 \text{g}^{-1}$		Pore diameter D_p , nm
		General	Micropores	
CMK-1	1245	0.78	0.40	3.4
CMK-3	1333	1.04	0.04	3.8
CMK-1_N	375	0.21	0.17	3.4
CMK-3_N	398	0.22	0.19	3.4
CMK-1_Pd	848	0.63	0.23	3.4
CMK-3_Pd	839	0.77	0.05	3.8
CMK-1_N_Pd	277	0.19	0.12	3.4
CMK-3_N_Pd	332	0.21	0.15	3.4
CMK-3_Pd_IL	575	0.53	0	4.1

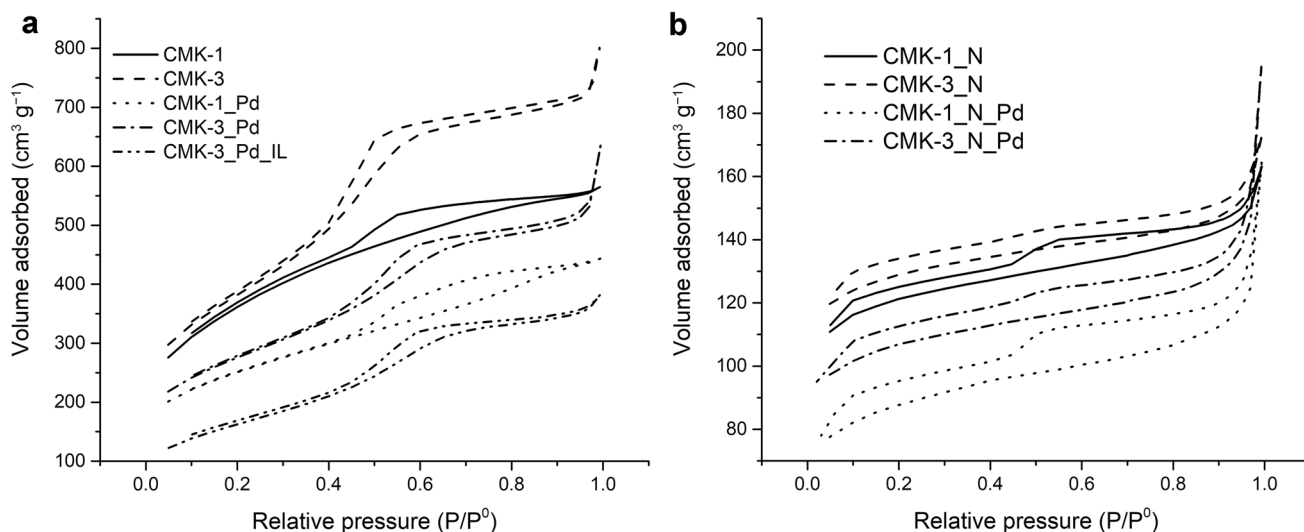


Fig. 1 Low-temperature adsorption–desorption isotherms of nitrogen synthesized carbon materials: **a** nitrogen undoped, **b** nitrogen doped

formed during the surface carbonization process. In addition, CMK-3 has a larger total pore volume compared to CMK-1. In the case of sample CMK-1, micropores account for almost half of the total pore volume.

When carbon materials are doped with nitrogen, the surface area reduces by almost 3 times. According to the studies of the authors [25], the carbon layer obtained from polyaniline covers both the outer and inner surfaces of the porous CMK structure, which leads to a decrease in the surface area.

Significant differences in pore size distribution can be observed for non-doped and doped samples. Thus, samples

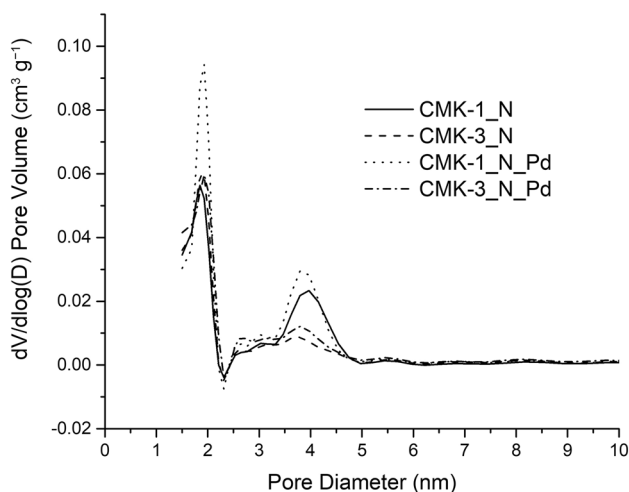


Fig. 2 Pores distribution of the studied carbon materials by diameter

CMK-1_N and CMK-3_N are characterized by a narrow pore size distribution with an average size of 2 nm (Fig. 2). Moreover, the main volume of pores falls precisely on micropores (80–85% of the total pore volume), which was formed as a result of carbonization of the carbon precursor [29].

Upon metal deposition, the S_{BET} values for all samples decreased: for non-doped samples—by 32–37%, for N doped—by 17–25% [30]. In the case of modification of the palladium-containing catalyst CMK-3_Pd with an ionic liquid, the surface area decreases by almost 1.5 times.

The presence of palladium in the synthesized catalysts was confirmed by *X-ray* fluorescence analysis (*XRF*), and the results are shown in Fig. 3.

XRF spectrum for all palladium-containing catalyst samples contains only characteristic signals of electronic transitions for palladium.

The Raman spectra shown in Fig. 4 provide additional information on the surface of synthesized carbon materials. As shown, the D band at about 1300 cm^{-1} and the G band at 1590 cm^{-1} characterize the disordered carbon and graphite carbon peak, respectively [31, 32]. The non-doped CMK-1 and CMK-3 are characterized by approximately the same ID/IG ratios (0.68 and 0.70, respectively). The insertion of nitrogen atoms into the carbon lattice is usually accompanied by the creation of defects. Therefore, for the doped samples CMK-1_N and CMK-3_N, a higher ID/IG ratio is observed, which implies a less ordered structure. Moreover, the CMK-1_N sample is characterized by a higher ratio (ID/IG = 0.82) compared to CMK-3_N (ID/IG = 0.72), which is

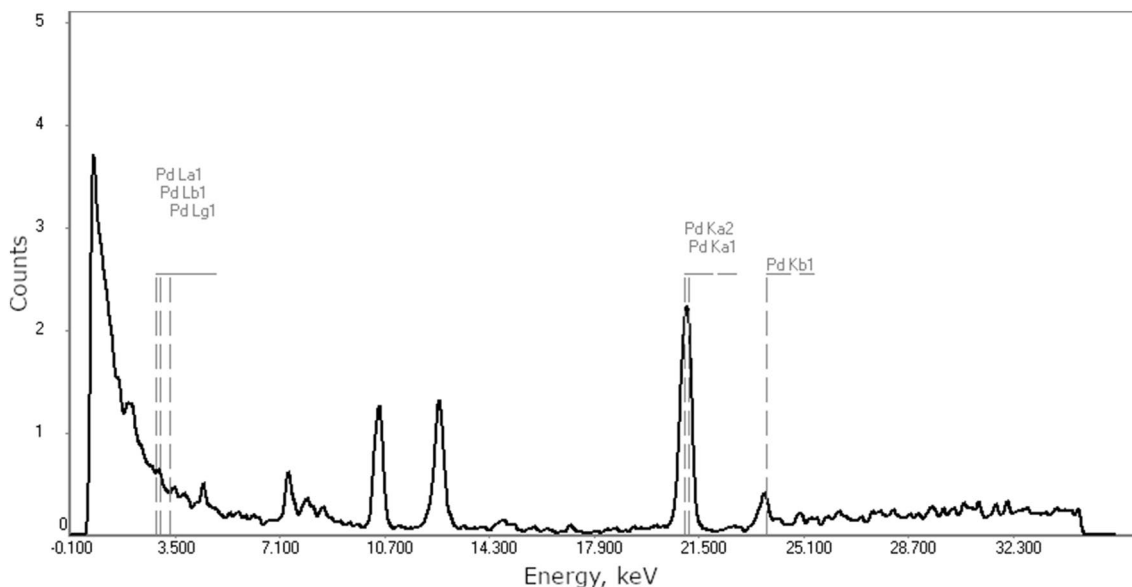


Fig. 3 Typical XRF spectrum of palladium-containing CMK samples

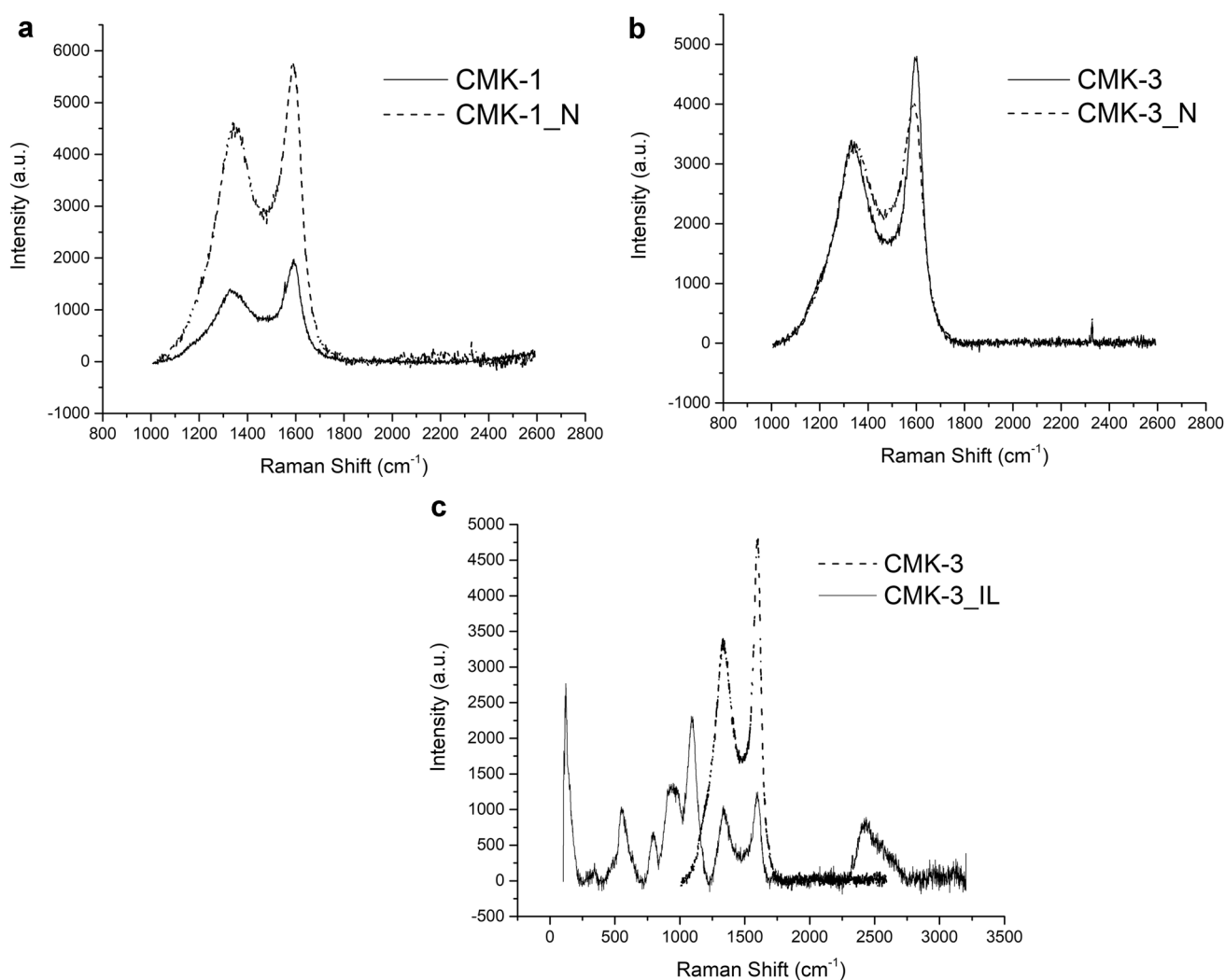


Fig. 4 Raman spectra of synthesized carbon materials: **a** CMK-1 doped and undoped with nitrogen, **b** CMK-3 doped and undoped with nitrogen, **c** modified with ionic liquid and unmodified CMK-3

associated with the presence of a larger number of defects and edge atoms.

Figure 4 shows Raman spectra of CMK-3 modified by ionic liquid [BMIM][Br]. The high-frequency range, $2800–3200\text{ cm}^{-1}$, exhibits a complex pattern of overlapped bands proper to several C–H stretching modes. The $800–1600\text{ cm}^{-1}$ range includes characteristic bands of imidazolium ring vibrations. The $400–800\text{ cm}^{-1}$ range also contains ring vibrations, which provides insight on conformations of alkyl chains [33].

The temperature-programmed reduction (TPR) curves of palladium-containing catalysts are shown in Fig. 5.

Analysis of the TPR data for Pd catalysts (Fig. 5 shows the profiles only for CMK-3_Pd and CMK-3_N_Pd) showed that the catalysts are completely reduced at 350 °C .

Therefore, this temperature was used to activate (reduce) the samples before testing the catalytic activity. On TPR profiles for palladium catalysts supported on CMK-3 and CMK-3_N, should be noted the presence of a small negative peak at about 80 °C . A similar release of H_2 in the temperature range of $50–100\text{ °C}$ is attributed to the decomposition of β -palladium hydride formed during TPR analysis [34]. The maximum absorption of hydrogen occurs at a temperature of 150 °C , which indicates that PdO particles on these catalysts are easily reduced at relatively low temperatures [35].

Thermal decomposition of the synthesized Pd-containing catalysts was investigated using combined differential thermal and thermogravimetric analysis. Two well-distinguishable regions of the materials mass loss can be distinguished on the curves (Fig. 6): in the temperature range of

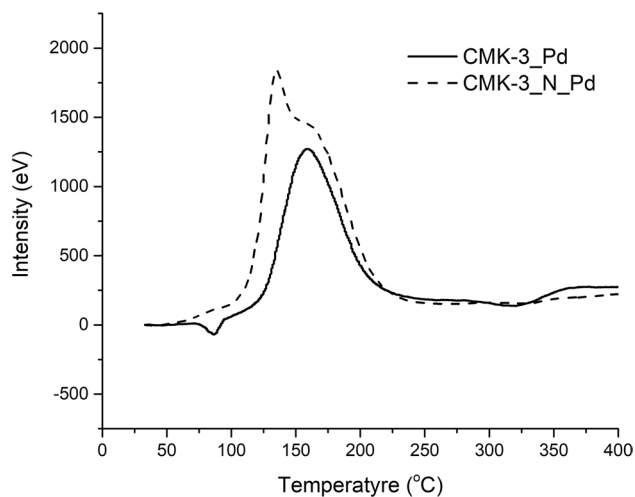


Fig. 5 The temperature-programmed reduction (TPR) curves of palladium-containing catalysts

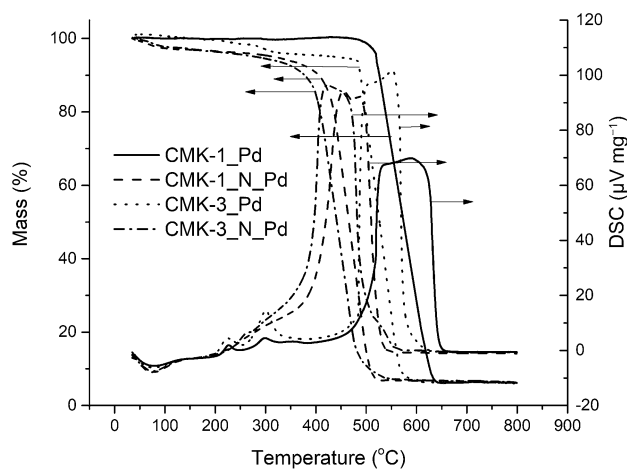


Fig. 6 The curves of combined differential thermal and thermogravimetric analysis of Pd-containing catalysts

100–120 °C and 400–600 °C. The insignificant weight loss observed in the range of 100–120 °C and mainly associated with the desorption of water from the surface and pores of the support. The main weight loss was observed in the temperature range of 400–600 °C due to oxidation of the carbon support (Fig. 6). At temperatures above 600 °C, no further weight loss was observed for the samples. The residual mass after analysis was 5%.

According to differential scanning calorimetry (DSC) data, in air atmosphere, exothermic reactions caused by carbon oxidation were observed for all samples. For samples on CMK-1, peak DSC temperatures were observed at ~450 °C, and for catalysts on CMK-3 at ~550 °C. The

higher oxidation temperature for the samples deposited on CMK-3 indicates a higher stability of its structure [36].

3.2 Electrochemical experiment

The electrochemical experiment was carried out in the modes of linear and cyclic voltammetry. Figure 7 shows linear voltammograms for synthesized CMK samples obtained using a rotating disk electrode.

Table 2 shows some characteristics of the oxygen electroreduction reaction from an alkaline electrolyte calculated based on the polarization curves.

It was found that the texture of CMK and the method of their modification strongly affect the activity of the process of oxygen electroreduction. The CMK-3_Pd catalyst, characterized by long channels of interconnected pores (2D hexagonal mesostructure with morphology of interconnected rods), has the highest activity in the studied process compared to other synthesized catalysts, in particular, with the CMK-1_Pd catalyst. This can be predominantly associated with a well-ordered mesoporous structure, which ensures rapid diffusion of adsorbed oxygen from solution into the catalyst bulk and accelerating the process of electrochemical oxygen reduction. For the CMK-1_Pd catalyst characterized by a three-dimensional pore structure (3D cubic mesostructure), oxygen diffusion is likely to be hindered due to the low pore connectivity. This may be due to the fact that the volume of mesopores in CMK-3_Pd is higher than in CMK-1_Pd, which is also characterized by the presence of micropores. Apparently, oxygen transport through the larger mesopores of the CMK-3_Pd catalyst is more intense, which leads to an increased activity of this catalyst in the reaction of oxygen electroreduction. It is likely that the participation of micropores in the transport of oxygen into the bulk of catalysts of the CMK type will be less expressed.

Doping with nitrogen did not lead to a significant increase in the activity in the studied reaction on the investigated mesoporous carbon catalysts. Moreover, the activities for the CMK-1_Pd and CMK-1_N_Pd catalysts are comparable—the difference between the initial potentials and the half-wave potentials is about 0.02 V. The diffusion current at potentials lower than -0.6 V is higher for the nitrogen-doped CMK-1_N_Pd catalyst; at a potential of -0.8 V, the difference in the values of the diffusion current for CMK-1_Pd and CMK-1_N_Pd is 0.26 mA cm^{-2} . The activity of CMK-3_Pd is significantly higher than for CMK-3_N_Pd—the difference between the initial potentials and half-wave potentials is about 0.04 and 0.09 V, respectively. At a potential of -0.8 V, the difference in the values of the diffusion current for CMK-3_Pd and CMK-3_N_Pd is 0.42 mA cm^{-2} . Thus, the doping of these materials with nitrogen by pyrolysis of polyaniline leads to blocking of pores and impairment of the

Fig. 7 Polarization curves for O₂ reduction on electrode with various catalysts in air-saturated KOH solution with a concentration 0.1 M: potential scan rate 5 mV s⁻¹, electrode rotating rate: 1000 rpm, catalyst loading: 80 μg cm⁻²

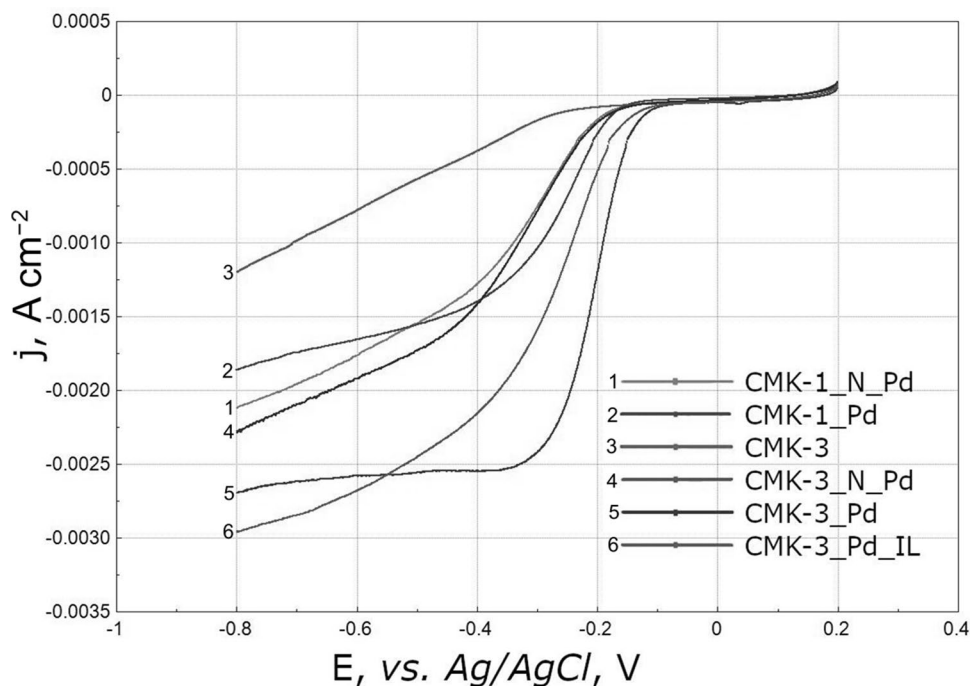


Table 2 Parameters for ORR on synthesized catalysts in KOH solution (O₂ saturated, 1000 rpm)

Catalysts	$j_{\text{dif}}(-0.8 \text{ V}), \text{ mA cm}^{-2}$	$E_{1/2}, \text{ V}$	$E_{\text{onset}}, \text{ V}$
CMK-3_Pd	2.70	-0.20	-0.07
CMK-3_Pd_IL	2.96	-0.23	-0.08
CMK-1_Pd	1.86	-0.25	-0.12
CMK-1_N_Pd	2.12	-0.27	-0.11
CMK-3_N_Pd	2.28	-0.29	-0.11
CMK-3	1.20	-0.38	-0.23

adsorbed oxygen transport into the bulk of the catalysts. This leads to a decrease in the activity of nitrogen-doped CMCs in the oxygen electroreduction reaction from an alkaline electrolyte. This is more typical for a CMK-3 type catalyst.

In the present study, the effect of an imidazolium ionic liquid ([BMIM][Br]) on the activity of catalysts of the CMK type in the oxygen reduction reaction was studied. It is shown that IL highly effects the process of oxygen electroreduction and is significantly superior materials doped with nitrogen. It was found that the doped sample CMK-3_N_Pd is less active in the studied reaction than the sample CMK-3_Pd_IL modified with an ionic liquid; the difference between $E_{1/2}$ and E_{onset} for these catalyst samples is 0.06 and 0.03 V, respectively. Although the activity of CMK-3_Pd_IL is reduced relative to the unmodified sample CMK-3_Pd (comparing the values of $E_{1/2}$ and E_{onset}). The diffusion current at potentials lower than -0.6 V is higher

for the catalyst CMK-3_Pd_IL modified with an ionic liquid; at a potential of -0.8 V, the difference in the values of the diffusion current for CMK-3_Pd and CMK-3_Pd_IL is 0.26 mA cm⁻². Apparently, the π -electronic structure of imidazole in the structure of the ionic liquid, in general, can increase the efficiency of the oxygen reduction process by increasing the electron density on the catalyst surface. However, for a more accurate mechanism of IL action on the process of oxygen electroreduction, additional theoretical and experimental studies are required.

Figure 8 shows the linear voltammetry for the most active catalysts CMK-3_Pd (a) and CMK-3_Pd_IL (b) at different speeds of rotation of the disk electrode.

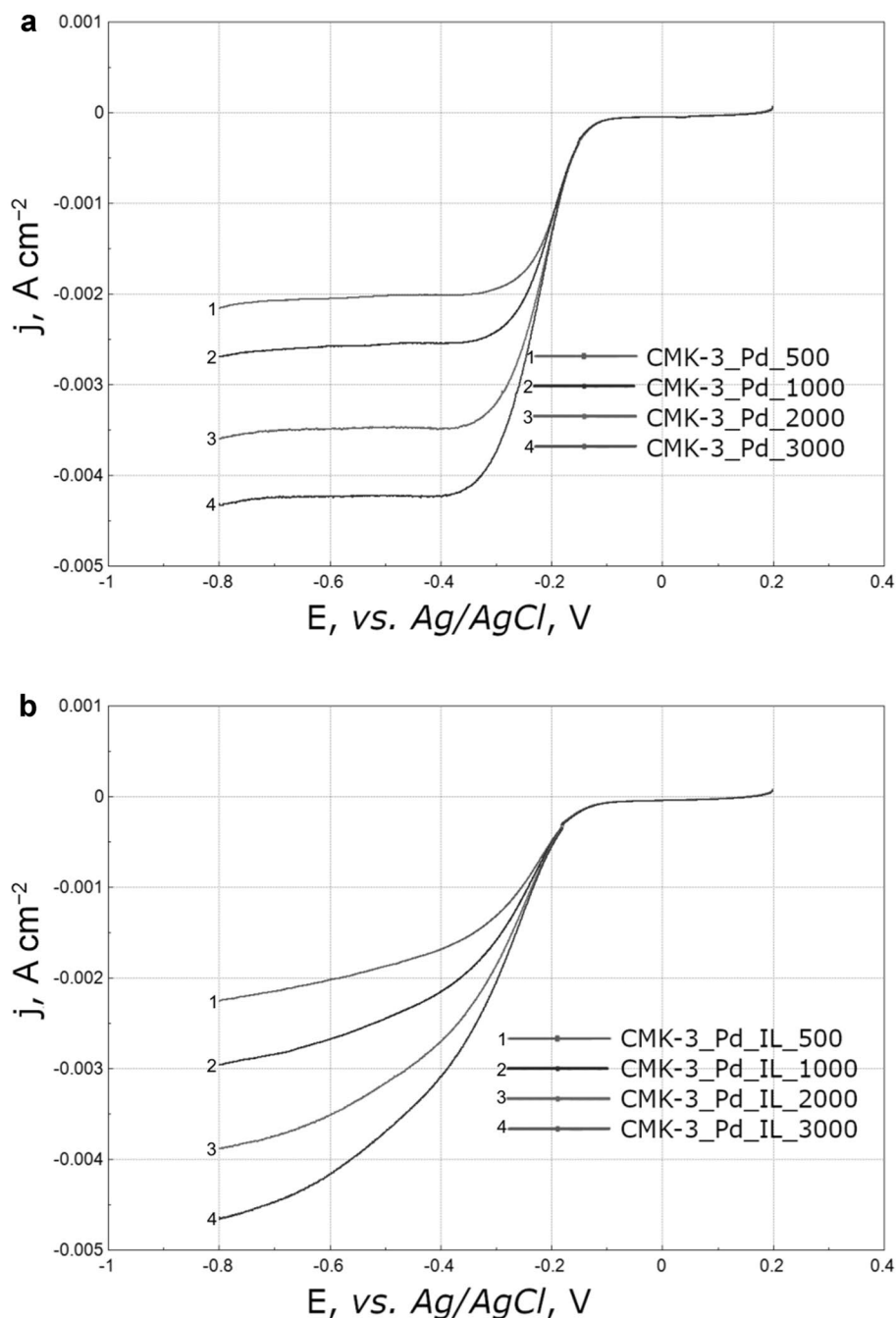
To compare the activity of the catalysts, the Koutecky-Levich equation was used, written in the following form [37, 38]:

$$\frac{1}{j} = \frac{1}{j_k} + \frac{1}{j_d} = \frac{1}{nFkC_{O_2}} + \frac{1}{0.62nFD_{O_2}^{2/3} \nu^{-1/6} C_{O_2} \omega^{1/2}},$$

where j is the measured current density, j_k and j_d are the kinetic and diffusion-limited current densities, respectively, k is the electrochemical rate constant for O₂ reduction, D_{O_2} —is the diffusion coefficient of oxygen (1.910–5 cm² s⁻¹), C_{O_2} —is the concentration of oxygen in the bulk (1.2 · 10⁻³ mol L⁻¹), ν is the kinematic viscosity of the solution (0.01 cm² s⁻¹), ω is the electrode rotation rate, and n is the number of electrons transferred per O₂ molecule.

Figure 9 shows the dependences in the coordinates of the Koutecky-Levich equation for all synthesized catalysts, obtained from the data on oxygen reduction at different

Fig. 8 Polarization curves of the reduction of O₂ on the electrode with CMK-3_Pd (a) and CMK-3_Pd_IL (b) at different electrode rotating rates (500, 1000, 2000, 3000 rpm) in an O₂-saturated KOH solution with a concentration of 0.1 M: potential sweep rate 5 mV s⁻¹, catalyst load: 80 μg cm⁻²



speeds of rotation of the disk electrode in a 0.1 M KOH solution with O₂-saturated.

Figure 10 shows the dependence of the number (n) of electrons transferred in the reaction on the value of the potential using the synthesized catalysts.

The dependences in the coordinates of the Koutetsky-Levich equation have a linear form, which indirectly confirm the diffusion-limiting stage of the oxygen electroreduction process. It has been shown that, on the CMK-3_Pd and CMK-3_Pd_IL catalysts, the electroreduction of oxygen at a potential of -0.8 V is characterized by a number of

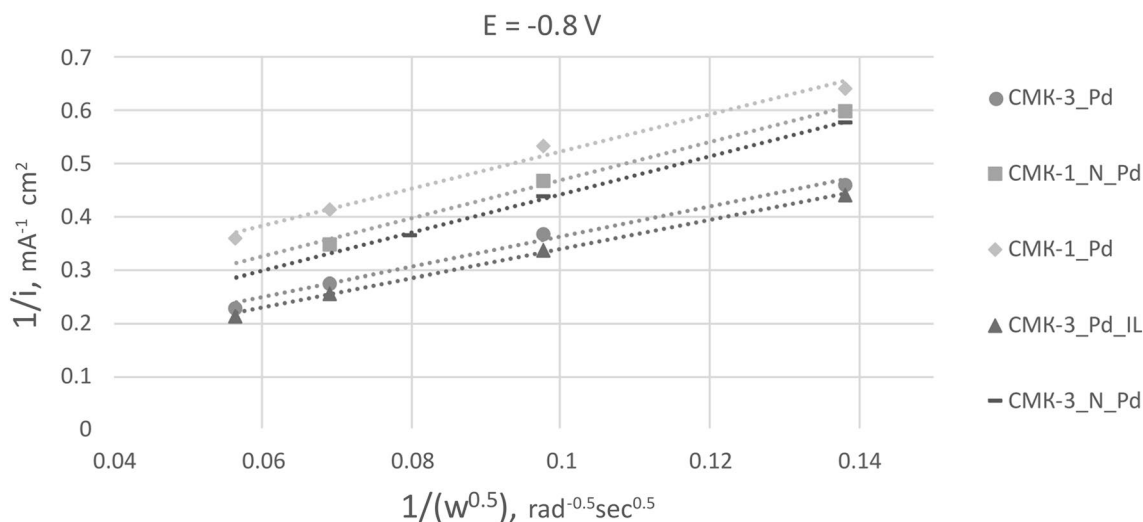


Fig. 9 Dependences in the coordinates of the Koutecky-Levich equation at the potential -0.8 mV for all catalyst samples

transferred electrons of about 3.5. This indicates a low yield of a by-product in the form of an HO_2^- ion and a predominant production of water in the process of the oxygen electroreduction reaction. When the potential is shifted to a more positive region, the number of electrons participating in the reaction decreases to 3 and the probability of the formation of the HO_2^- increases. For other investigated catalysts, in particular, doped with nitrogen, the mechanism is close to the 2-electron process at all investigated potentials, so the oxygen reduction process on them will be carried out through the intermediate formation of hydrogen peroxide. It has been shown that on the CMK-3_Pd and CMK-3_Pd_IL

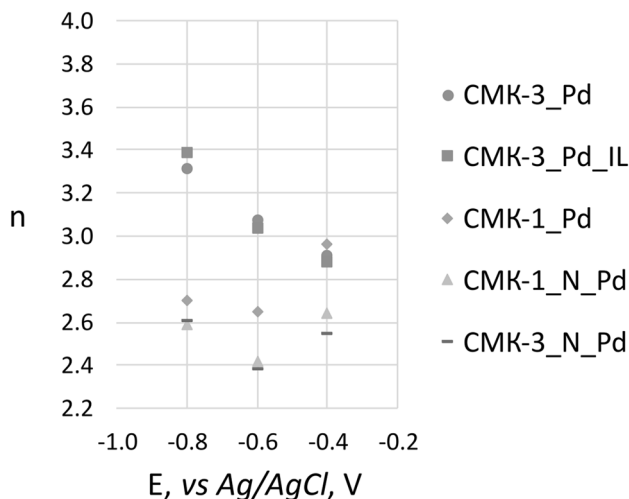


Fig. 10 The calculated numbers of electrons transferred in the reaction from the value of the potential

catalysts, the limiting current at -0.8 V and 3000 rpm reaches 4.4 and 4.7 mA/cm^2 , respectively.

The type of cyclic voltammograms (Fig. 11) indicates that the texture and method of CMK modification significantly affect the values of the specific electrochemical active surface.

Q_c (C cm^{-2}) is the amount of electricity required to charge the surface of the studied material, which was determined from the cathode region of the CVs using the following formula [39]:

$$Q_{\text{catod}} = \frac{\int idE}{\vartheta},$$

where ϑ —the potential scan rate (V s^{-1}) parameter Q_{catod} is a characteristic of electrochemical active surface values (S_{EAS}).

It was found that doping CMK-1_Pd with nitrogen leads to an increase in the active electrochemical surface. For CMK-3_Pd, on the contrary, a decrease in the size of the active surface is observed upon doping with nitrogen. The electrochemical surface modified by the ionic liquid also slightly decreases. It can be assumed that the activity of materials based on CMK in the reaction of oxygen electroreduction from an alkaline electrolyte will depend not only on the number of active centers (proportional to S_{EAS} , presented in Table 3) on the surface, but also on the textural characteristics of the materials.

Figure 12 shows the voltammograms for the most efficient catalysts in this study and a commercial platinum catalyst with a mass content of platinum of 20%.

Fig. 11 Cyclic voltammogram (CV) on electrode with various catalysts in de-aerated 0.1 M KOH solution: potential scan rate 50 mV s^{-1}

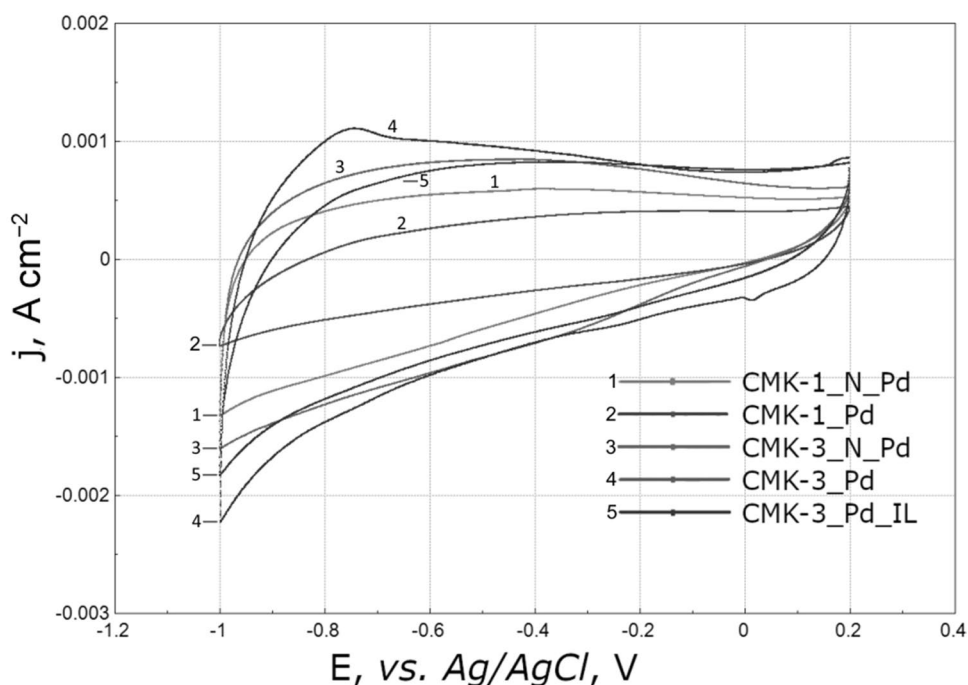


Table 3 Electrochemical active surface values (S_{EAS}) for the catalysts ($\theta=50 \text{ mV s}^{-1}$)

Catalyst	Q_c ((as S_{EAS}), mC cm^{-2})
CMK-3_Pd	20.80
CMK-3_Pd_IL	18.50
CMK-1_Pd	7.93
CMK-1_N_Pd	13.34
CMK-3_N_Pd	16.74

On the voltammograms of the catalysts, three regions for the reaction under study: the diffusion, mixed, and kinetic regions. Figure 13 shows comparative diagrams of specific (j) and mass activity (i) activity in the diffusion and kinetic regions for CMK-3_Pd, CMK-3_Pd_IL, and Pt/C.

The mass activity of the CMK-3_Pd and CMK-3_Pd_IL catalysts in the diffusion region at a potential (-0.8 V) is significantly higher than that of commercial Pt/C. In the kinetic region at a potential (-0.05 V), the mass activity is higher for the platinum catalyst, but the values are comparable. This is probably due to the high dispersion of palladium on the mesoporous matrix CMK-3 and CMK-3 modified with an ionic liquid. The specific activity in the kinetic region is significantly higher for the platinum catalyst as compared to the synthesized palladium catalysts based on CMK, which is associated with a high content of platinum (20 wt%) in the Pt/C catalyst. In the diffusion region, these quantities are comparable.

Thus, the synthesized catalysts based on CMK-3 can be further tested as a cathode electrode in alkaline fuel cells. A large load of palladium will be required to enhance the activity, as well as some modification of the CMK-3 surface, in particular, functionalization with ionic liquids.

The most active catalyst CMK-3_Pd was tested for corrosion resistance by running 1000 cycles in a stream of oxygen. After cycling, a linear voltammogram was taken and the diffusion current was calculated at a potential -0.80 V . (Fig. 14).

After 1000 cycles in an oxygen atmosphere, the current density in the diffusion region for the CMK-3_Pd catalyst decreases by $\sim 2.2\%$, which indicates a high corrosion resistance of material in the studied process.

Table 4 compares the characteristics of the studied reaction obtained in this work with the literature data.

It can be seen that the synthesized bimetallic catalysts on CMK-3 are characterized by $E_{1/2}$ and E_{onset} characteristics comparable with some obtained in similar studies.

4 Conclusions

Catalysts for the electrochemical reduction of oxygen from an alkaline electrolyte based on mesoporous carbon materials CMK-1 and CMK-3 have been synthesized. It was found that the doping of carbon material based on CMK-1 with nitrogen by pyrolysis of polyaniline leads to an increase in the diffusion current for the palladium-containing catalyst CMK-1_N_Pd compared to CMK-1_Pd. For catalysts

Fig. 12 Voltammograms for the most active catalysts based on CMK and a commercial platinum catalyst: potential scan rate 5 mV s^{-1} , electrode rotating rate: 1000 rpm, catalyst loading: 80 mkg cm^{-2}

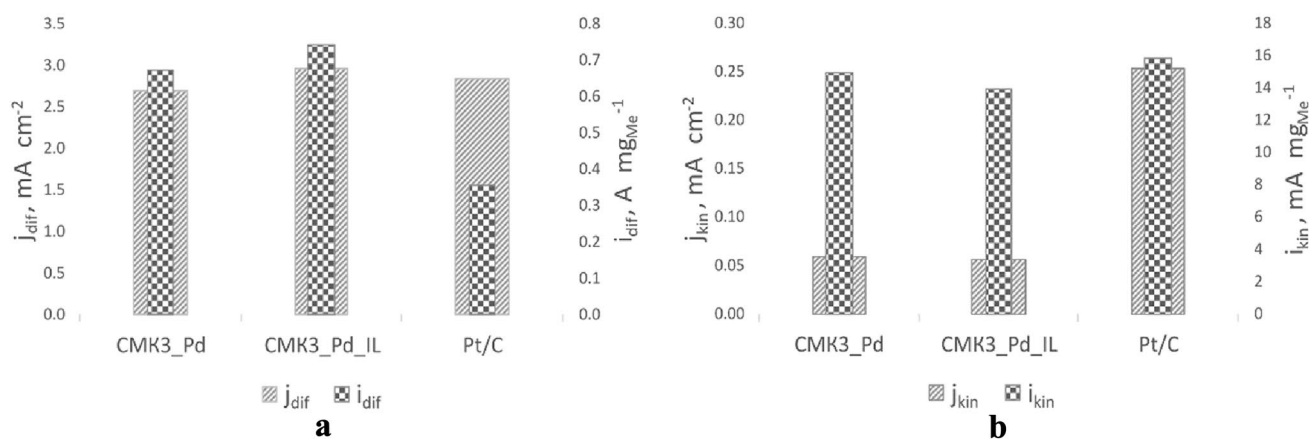
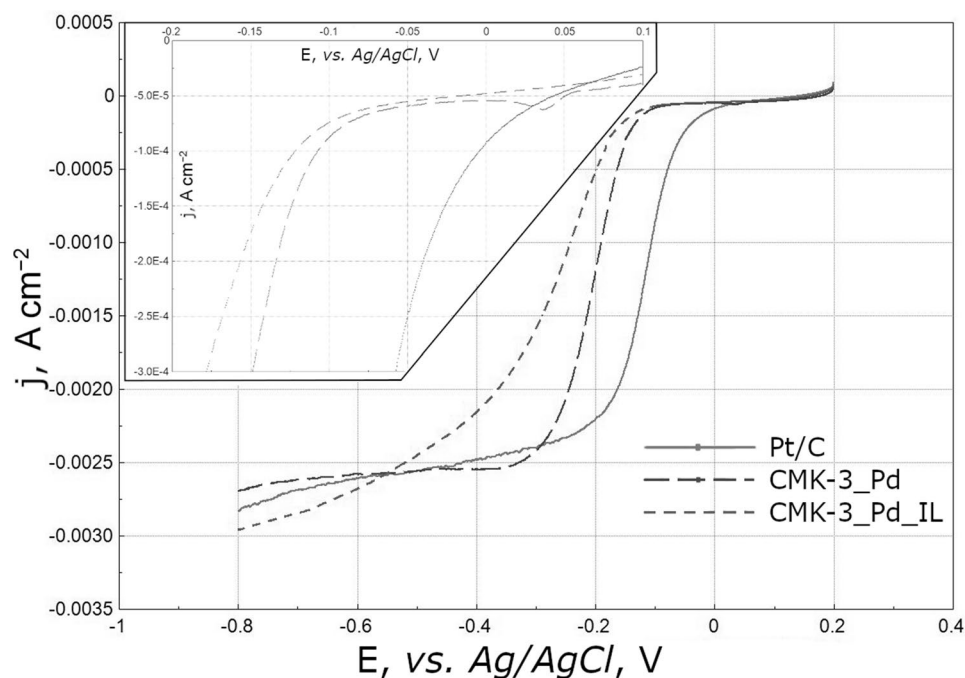


Fig. 13 Comparative diagrams of the specific and mass activities of catalysts in the kinetic (a) and diffusion (b) regions

based on CMK-3 doped with nitrogen, on the contrary, the efficiency of electrochemical oxygen reduction process is reduced from an alkaline electrolyte. It could be concluded that doping of this material with nitrogen leads to the blocking of pores and, thereafter, the transport of adsorbed oxygen into the catalyst volume worsens. It was found that IL ([BMIM] [Br]) generally favorably affects the process of oxygen electroreduction and is significantly superior in this respect to materials doped with nitrogen. The electroreduction of oxygen from an alkaline electrolyte at a potential of -0.8 V is characterized by a number of transferred electrons of about 3.5 on the CMK-3_Pd and CMK-3_Pd_IL catalysts. Other synthesized catalysts, in particular, doped

with nitrogen, are characterized by a mechanism close to the 2-electron process at all investigated potentials. Moreover, the activity of materials based on CMK in the reaction of oxygen electroreduction from an alkaline electrolyte will depend not only on the size of the electrochemically active surface of the catalysts, but also on the textural characteristics of these materials. The mass activity of the CMK-3_Pd and CMK-3_Pd_IL catalysts in the kinetic region is comparable to the activity of the Pt/C platinum catalyst, which is probably due to the high dispersion of palladium on the CMK-3 matrix. The specific activity of the catalysts in the kinetic region is much higher for the platinum catalyst. In the diffusion region at a potential of -0.8 V , the mass activity of

Fig. 14 Corrosion resistance test of the CMK-3_Pd catalyst: LV before and after 1000 cycles

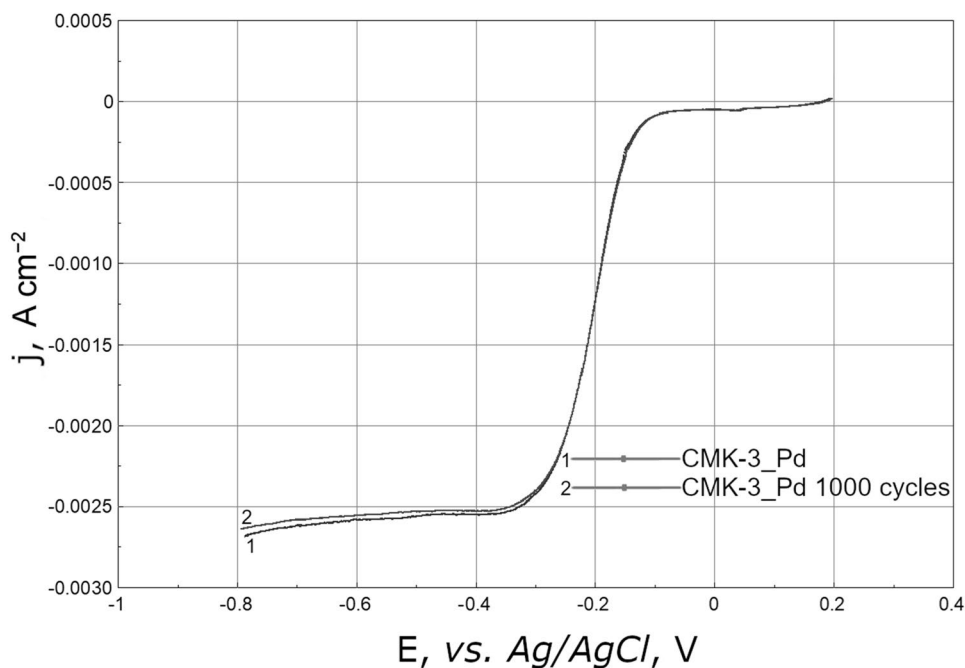


Table 4 Comparison of characteristics obtained in present work with literature data

Catalyst	$E^{1/2}$, V	E_{onset} , V	Source
CMK-3_Pd	-0.20	-0.07	This work
CMK-3_Pd_IL	-0.23	-0.08	This work
Pd@Ag/RGO	-0.17	0.183	[40]
Nanofetpc-s-MWCNT	-0.40	-0.200	[41]

the CMK-3_Pd and CMK-3_Pd_IL catalysts is almost two times higher than that of the platinum catalyst at comparable specific activity values.

Author contributions All authors contributed to the study conception and design. Material preparation, data collection, and analysis were performed by EAM, SVV, RVS, KYV, EOT, AVB, and HZ. The first draft of the manuscript was written by EAM, SVV, and RVS, and all authors commented on previous versions of the manuscript. All authors read and approved the final manuscript.

Funding The study was carried out with the financial support of the Russian Foundation for Basic Research and the BRICS framework program in the field of STI No.51961145107 according to the research project Grant No. 19–53–80033.

Declarations

Conflict of interest The authors declared that they have no conflict of interest.

References

- Daud WRW, Rosli RE, Majlan EH, Hamid SAA, Mohamed R, Husaini T (2017) PEM fuel cell system control: a review. *Renew Energ* 113:620–638
- Wang Y, Diaz DFR, Chen KS, Wang Z, Adroher XC (2020) Materials, technological status, and fundamentals of PEM fuel cells—a review. *Mater Today* 32:178–203
- Zeng WJ, Tong L, Liu J, Liang HW (2022) Annealing-temperature-dependent relation between alloying degree, particle size, and fuel cell performance of PtCo catalysts. *J Electroanal Chem* 922:116728
- Jung WS, Kim T, Popov BN (2022) Development of highly active and stable catalyst supports and platinum-free catalysts for PEM fuel cell. *J Electrochem Soc.* <https://doi.org/10.1149/1945-7111/ac7827>
- Chandran P, Ghosh A, Ramaprabhu S (2018) High-performance platinum-free oxygen reduction reaction and hydrogen oxidation reaction catalyst in polymer electrolyte membrane fuel cell. *Sci Rep* 8:3591. <https://doi.org/10.1038/s41598-018-22001-9>
- Tarasevich MR, Davydova ES (2016) Nonplatinum cathodic catalysts for fuel cells with alkaline electrolyte. *Russ J Electrochem* 52:193–219
- Wang W, Wang Z, Wang J, Zhong CJ, Liu CJ (2017) Highly active and stable Pt–Pd alloy catalysts synthesized by room-temperature electron reduction for oxygen reduction reaction. *Adv sci* 4:1600486
- Maiyalagan T, Alaje TO, Scott K (2012) Highly stable Pt–Ru nanoparticles supported on three-dimensional cubic ordered mesoporous carbon (Pt–Ru/CMK-8) as promising electrocatalysts for methanol oxidation. *J Phys Chem C* 116:2630–2638
- Ruiz-García C, Heras F, Calvo L, Alonso-Morales N, Rodríguez JJ, Gilarranz MA (2019) N-doped CMK-3 carbons supporting palladium nanoparticles as catalysts for hydrodechlorination. *Ind Eng Chem Res* 58:4355–4363
- Tan X, Zhang J, Wu X, Wang Y, Li M, Shi Z (2018) Palladium nanoparticles loaded on nitrogen and boron dual-doped

- single-wall carbon nanohorns with high electrocatalytic activity in the oxygen reduction reaction. *RSC Adv* 8:33688–33694
11. Zhu H, Zhang S, Huang YX, Wu L, Sun S (2013) Monodisperse $M_xFe_{3-x}O_4$ ($M = Fe, Cu, Co, Mn$) nanoparticles and their electrocatalysis for oxygen reduction reaction. *Nano Lett* 13:2947–2951
 12. Guo C, Li Y, Li Z, Liu Y, Si Y, Luo Z (2020) Nanochannel-controlled synthesis of ultrahigh nitrogen-doping efficiency on mesoporous Fe/N/C catalysts for oxygen reduction reaction. *Nanoscale Res Lett* 15:1–14
 13. Zaitseva YN, Novikova SA, Parfenov VA, Vyatkin AS, Ryzhkov II (2019) Synthesis and electrochemical properties of CMK-3 with particles of nickel, cobalt and copper. *J Siberian Federal Univ Chem* 12:395–404
 14. Vij V, Sultan S, Harzandi AM, Meena A, Tiwari JN, Lee WG, Kim KS (2017) Nickel-based electrocatalysts for energy-related applications: oxygen reduction, oxygen evolution, and hydrogen evolution reactions. *ACS Catal* 7:7196–7225
 15. Zhao Y, Chu Y, Ju X, Zhao J, Kong L, Zhang Y (2018) Carbon-supported copper-based nitrogen-containing supramolecule as an efficient oxygen reduction reaction catalyst in neutral medium. *Catalysts* 8:53
 16. Patil RB, Mantri A, House SD, Yang JC, McKone JR (2019) Enhancing the performance of Ni-Mo alkaline hydrogen evolution electrocatalysts with carbon supports. *ACS Appl Energy Mater* 2:2524–2533
 17. Laszczyńska A, Tylus W, Szczygieł I (2021) Electrocatalytic properties for the hydrogen evolution of the electrodeposited Ni-Mo/WC composites. *Int J Hydrog Energy* 46:22813–22831
 18. Sun J, Li S, Zhang Q, Guan J (2020) Iron-cobalt-nickel trimetal phosphides as high-performance electrocatalysts for overall water splitting. *Sustain Energy Fuels* 4:4531–4537
 19. Eftekhari A, Fan Z (2017) Ordered mesoporous carbon and its applications for electrochemical energy storage and conversion. *Mat Chem Front* 1:1001–1027. <https://doi.org/10.1039/C6QM00298F>
 20. Xu W, Wu Z, Tao S (2016) Recent progress in electrocatalysts with mesoporous structures for application in polymer electrolyte membrane fuel cells. *J Mat Chem A* 4:16272–16287. <https://doi.org/10.1039/C6TA05304A>
 21. Hasse B, Gläsel J, Kern AM, Murzin DY, Etzold BJM (2015) Preparation of carbide-derived carbon supported platinum catalysts. *Catal Today* 249:30–37. <https://doi.org/10.1016/j.cattod.2014.10.049>
 22. Wang Y, Liu Y, Li XZ, Zeng F, Liu H (2013) A highly-ordered porous carbon material based cathode for energy-efficient electro-fenton process. *Sep Purif Technol* 106:32–37. <https://doi.org/10.1016/j.seppur.2012.12.013>
 23. Zhao Z, Li M, Zhang L, Dai L, Xia Z (2015) Design principles for heteroatom-doped carbon nanomaterials as highly efficient catalysts for fuel cells and metal-air batteries. *Adv Mater* 27:6834–6840. <https://doi.org/10.1002/adma.201503211>
 24. Kado Y, Soneda Y, Hatori H, Kodama M (2019) Advanced carbon electrode for electrochemical capacitors. *J Solid State Electrochem* 23:1061–1081. <https://doi.org/10.1007/s10008-019-04211-x>
 25. Wu D, Lou Z, Wang Y, Xu T, Shi Z, Xu J, Li X (2017) Construction of MoS₂/Si nanowire array heterojunction for ultrahigh-sensitivity gas sensor. *Nanotechnology* 28:435503. <https://doi.org/10.1088/1361-6528/aa89b5>
 26. Song S, Qin T, Li Q, Wang Y, Tang Y, Zhang L, Liu X (2021) Single Co atoms implanted into N-doped hollow carbon nanoshells with non-planar Co-N₄-1-O₂ sites for efficient oxygen electrochemistry. *Inorganic Chemistry* 60:7498–7509. <https://doi.org/10.1021/acs.inorgchem.1c00824>
 27. Han B, Yu S, Wang Z, Zhu H (2020) Imidazole polymerized ionic liquid as a precursor for an iron-nitrogen-doped carbon electrocatalyst used in the oxygen reduction reaction. *Int J Hydrog Energy* 45:29645–29654. <https://doi.org/10.1016/j.ijhydene.2019.09.123>
 28. Beck JS, Vartuli JC, Roth WJ, Leonowicz ME, Kresge CT, Schmitt KD, Schlenker J (1992) A new family of mesoporous molecular sieves prepared with liquid crystal templates. *J Am Chem Soc* 114:10834–10843
 29. Liu Y, Li Z, Yang X, Xing Y, Tsai C, Yang Q, Yang RT (2016) Performance of mesoporous silicas (MCM-41 and SBA-15) and carbon (CMK-3) in the removal of gas-phase naphthalene: adsorption capacity, rate and regenerability. *RSC Adv* 6:21193–21203. <https://doi.org/10.1039/C5RA27289K>
 30. Calvillo L, Gangeri M, Perathoner S, Centi G, Moliner R, Lázaro MJ (2011) Synthesis and performance of platinum supported on ordered mesoporous carbons as catalyst for PEM fuel cells: effect of the surface chemistry of the support. *Int J Hydrog Energy* 36:9805–9814. <https://doi.org/10.1016/j.ijhydene.2011.03.023>
 31. Makal TAD, Li JR, Lu W, Zhou HC (2021) Methane storage in advanced porous materials. *Zhou Chem Soc Rev* 41(23):7761–7779
 32. Jeon IY, Noh HJ, Baek JB (2020) Nitrogen-doped carbon nanomaterials: synthesis, characteristics and applications. *Chem Asian J*. <https://doi.org/10.1002/asia.201901318>
 33. Lima TA, Faria LF, Paschoal VH, Ribeiro MC (2018) Communication: glass transition and melting lines of an ionic liquid. *J Chem Phys* 148:171101. <https://doi.org/10.1063/1.5030083>
 34. Ivashchenko NA, Gac W, Tertykh VA, Yanishpolskii VV, Khainakov SA, Dikhtiarenko AV, Zawadzki W (2012) Preparation, characterization and catalytic activity of palladium nanoparticles embedded in the mesoporous silica matrices. *World J Nano Sci Eng* 2:117. <https://doi.org/10.4236/wjnse.2012.23015>
 35. Arjmand M, Chizari K, Krause B, Pötschke P, Sundararaj U (2013) Application of photocatalysts and LED light sources in drinking water treatment. *Catalyst* 3:726–743. <https://doi.org/10.3390/catal3030726>
 36. Arjmand M, Chizari K, Krause B, Pötschke P, Sundararaj U (2016) Effect of synthesis catalyst on structure of nitrogen-doped carbon nanotubes and electrical conductivity and electromagnetic interference shielding of their polymeric nanocomposites. *Carbon* 98:358–372. <https://doi.org/10.1016/j.carbon.2015.11.024>
 37. Levich VG (1962) Physicochemical hydrodynamics. *J Electrochem Soc*. <https://doi.org/10.1149/1.2425619>
 38. Koutecky J, Levich VG (1958) The use of a rotating disk electrode in the studies of electrochemical kinetics and electrolytic processes. *Zh Fiz Khim* 32:1565–1575
 39. Bogdanovskaya V, Vernigor I, Radina M, Andreev V, Korchagin O, Novikov V (2020) Carbon nanotube modified by (O, N, P) atoms as effective catalysts for electroreduction of oxygen in alkaline media. *Catalysts* 10:892. <https://doi.org/10.3390/catal10080892>
 40. Raghavendra P, Reddy GV, Sivasubramanian R, Chandana PS, Sarma LS (2018) Reduced graphene oxide-supported Pd@Au bimetallic nano electrocatalyst for enhanced oxygen reduction reaction in alkaline media. *Int J Hydrog Energy* 43(8):4125–4135
 41. Fashedemi OO, Ozoemena KI (2015) Oxygen reduction reaction at MWCNT-modified nanoscale iron (II) tetrasulfophthalocyanine: remarkable performance over platinum and tolerance toward methanol in alkaline medium. *RSC Adv* 5(29):22869–22878

Publisher's Note Springer Nature remains neutral with regard to jurisdictional claims in published maps and institutional affiliations.

Springer Nature or its licensor (e.g. a society or other partner) holds exclusive rights to this article under a publishing agreement with the

author(s) or other rightsholder(s); author self-archiving of the accepted manuscript version of this article is solely governed by the terms of such publishing agreement and applicable law.